Performance Analysis and Enhancement for A Cooperative Wireless Diversity Network with Spatially Random Mobile Helpers

Peijian Ju[a], Wei Song[a,*], A-Long Jin[a], Dizhi Zhou[a]

[a]*Faculty of Computer Science, University of New Brunswick, Fredericton, Canada*

Abstract

In many studies on wireless cooperative diversity, it is often assumed that the number of helpers and their locations are deterministic or known *a priori*. In this paper, we relax such assumptions and investigate a wireless diversity system with distributed cooperation and spatially random helpers subject to random direction (RD) mobility. To enable opportunistic relaying with multiple helpers, we consider an ALOHA-like medium access control (MAC) scheme and a timer-based random backoff scheme for multi-helper coordination. Particularly, we analyze the upper bound of combined signal-to-noise ratio (SNR) and unconditional success probability with multi-helper cooperation. We also provide numerical approximations for the delay of the two MAC schemes. To characterize the tradeoff between the success probability and delay, we further define a success/delay ratio, which can be maximized by adapting the intensity of selected helpers. The numerical and simulation results validated the analysis accuracy and demonstrated insightful observations.

Keywords: Cooperative communications, wireless diversity, multiple helpers, relay selection, stochastic geometry, mobility

*Corresponding author. This research was supported by Natural Sciences and Engineering Research Council (NSERC) of Canada.

Email addresses: i1689@unb.ca (Peijian Ju), wsong@unb.ca (Wei Song), along.jin@unb.ca (A-Long Jin), q5frc@unb.ca (Dizhi Zhou)

1. Introduction

Due to the unique features such as path loss and fading, wireless links support a much less bandwidth than wired links. Although the multiple-input and multiple-output (MIMO) technology can exploit spatial diversity to improve wireless channel capacity, it is not feasible to integrate multiple antennas in palm-sized mobile terminals due to the constraints on size, weight and battery. In recent years, there was extensive research on cooperative communications [1, 2], which enable cooperation among mobile terminals to form virtual antennas and achieve spatial diversity via cooperation. Specifically, the cooperating helper nodes can relay the overheard signal from the source by various schemes, such as amplify-and-forward (AF) and decode-and-forward (DF). A variety of cooperative communication techniques were studied for wireless sensor networks [3], wireless local area networks [4], and wireless ad hoc networks [5].

Generally speaking, the cooperation among wireless nodes, which brings spatial diversity gain, can be performed in a centralized or distributed manner. In centralized cooperation, the source gathers the knowledge about the helpers and selects the best helper(s) for cooperation. The analysis of the diversity gain often needs certain *a priori* deterministic knowledge of the network, such as the number of helpers, and their locations and characteristics of received signal strength [6, 7, 8]. The collection of such knowledge is reasonable when the network topology is static. It becomes challenging, however, with a varying topology, e.g., when the nodes are moving and their locations are changing. In such circumstances, the received signal strength of helpers (e.g., the expectation of the received signal-to-noise ratio) presents dynamic variations which are related to the locations of helpers. Hence, the collected network knowledge can be out-of-date quickly with fast movements [9]. As a result, the selected relay may not be the best due to lack of accurate network information, which undermines the achievable cooperation gain at the physical layer and/or the media access control (MAC) layer. On the other hand, a distributed approach requires minimum *a priori* knowledge of the helpers and thus is robust to network variations.

Nonetheless, it is more complex to analyze the diversity gain of a distributed approach, especially in the case of multiple helpers where the spatial diversity gain of cooperation can be potentially high. From the physical-layer point of view, the more helpers, the higher the diversity gain. Meanwhile, more coordination delay may also be involved at the MAC layer. Hence, it is important to balance the tradeoff between the physical-layer diversity gain and MAC-layer delay.

Based on the above observations, this paper aims to address the following key questions:

- When the helpers are moving, the fading characteristics of the received signal strength is not static but varying with the node locations. In such a case, how can we analyze the diversity gain?
- Considering node mobility, the spatial distribution of potential helpers is random depending on the overheard signal quality. In particular, the number of potential helpers becomes a random variable. How can the spatially random distribution of helpers impact on the diversity gain?
- Intuitively, there is a tradeoff between the physical-layer diversity gain and MAC-layer delay when multiple helpers are available. Nonetheless, the exact scaling relationship depends on the spatial distribution of helpers. How can we mathematically quantify the tradeoff and obtain an optimal balance point in this tradeoff relationship?

To answer the above questions, we focus on a wireless diversity system with multiple helpers based on a distributed cooperation strategy. Each node independently decides to cooperate as a helper or not based on its local estimates of signal-to-noise ratio (SNR) between the source, the destination, and itself. As such, each node does not need to acquire a global knowledge of other helper candidates and their channel characteristics. Moreover, the potential helpers are assumed subject to random direction (RD) mobility [10]. As a result, the spatial distribution of helpers becomes random. Hence, we apply stochastic ge-

ometry [11, 12] to model the random locations of potential helper nodes and analyze the aggregate cooperative performance with multiple helpers. The key contributions of this paper are several-fold:

- Assume that all the nodes, except the source and the destination, are distributed as a Poisson point process (PPP). Considering the spatial random locations, we analyze the helper set with $p(x)$-*thinning* [11] and derive the exact form and approximation forms of the probability distribution of the upper bound of the total combined SNR.

- Based on the SNR upper bound, we further obtain the unconditional success probability of the multi-helper cooperation strategy. This is the probability that the received SNR is above a given threshold and it is also the complement of the outage probability. The success probability is proved to be approximately linear with the number of helpers and the helper intensity under certain conditions.

- To evaluate the tradeoff between the success probability and delay, we consider two medium access control (MAC) schemes to coordinate multiple helpers, i.e., an ALOHA-like scheme and a timer-based random backoff scheme. It is shown that the delay of the ALOHA scheme increases exponentially with the number of helpers, whereas the delay of the timer-based scheme increases more slowly. To characterize the tradeoff, we further define a success/delay ratio, which can be maximized by adapting the intensity measure of selected helpers.

The remainder of this paper is organized as follows. In Section II, we introduce the related work. The system model under study is defined in Section III. In Section IV, we present our analysis for the unconditional success probability, delay, outage-delay tradeoff and success/delay ratio. The numerical and simulation results in Section V validate the analysis accuracy and demonstrate the performance tradeoff. In Section VI, we conclude the paper and highlight some future research directions to extend this work.

2. Related Work

Cooperative wireless networks at the physical layer have been widely studied in the literature. The basic AF and DF relaying schemes were proposed and analyzed in [13], where maximum ratio combining (MRC) was considered at the destination node to obtain the total SNR. As the proposed form for the total SNR is very complicated, it is more tractable and feasible to apply an upper bound and lower bound in practice. A lower bound for the total SNR was proposed in [14], while an upper bound can be found in [14, 15]. Based on the total SNR expression, the conditional outage performance can be analyzed accordingly. In [6], the outage performance of cooperative relaying was evaluated for a Rayleigh fading and half-duplex channel in the low SNR regime. In [7, 16], a closed-form conditional outage probability of DF was derived for a Rayleigh fading and Nakagami-m fading channel, respectively. In [8], the probability density function (PDF) of the total SNR upper bound was proposed under both an $i.i.d$ and non-$i.i.d$ condition. The outage probability for each case was also derived correspondingly. However, the outage analysis in [8] is still conditional and further improved in [17] and [18]. The work in [17] considered that N strongest helpers are selected out of M candidates, although how to select them was not discussed. In [18], a dynamic scheme of selecting multiple helpers was proposed.

Cooperation at the MAC layer needs to address two important questions: 1) when to cooperate and 2) whom to cooperate with [19, 20]. If a single entity (e.g., the source) answers both questions, it is centralized cooperative MAC, such as [21]. Yang *et al.* in [21] propose a relay assignment scheme at the source and also consider helper incentive. A global optimal policy is designed to associate each source with a best relay so that the overall system capacity is maximized. On the other hand, a distributed cooperative MAC solution usually has the helper entities answer both questions in a decentralized fashion, e.g., [22]. The timer-based selection scheme proposed in [22] is based on the assumption that a helper with a shorter channel access time is preferable. Thus, the first responding helper is supposed to be the optimal helper. As such, no information

broadcast is necessary for the helpers to obtain knowledge of other competitors, which alleviates the network from broadcast traffic. Even though [21] and [22] are good cooperative MAC solutions, both focus on a static topology and single best helper assumption.

In the meantime, there has been little work in the literature that considers the tradeoff between the physical layer and the MAC layer for cooperative communications. The cross-layer solution in [22] did not address this tradeoff but only exploit the physical-layer parameters as criteria for helper selection at the MAC layer. The general tradeoff between power consumption at the physical layer and delay at the MAC layer are explored in [23] and [24], but they are not for the cooperative communication scenario. In this paper, we aim to analytically quantify the tradeoff between the physical-layer outage probability and the MAC-layer delay with cooperation among spatially random moving helpers.

Many existing studies on the cooperative diversity performance did not explicitly address the effect of the spatial distribution of helpers. The theory of stochastic geometry [11] provides a powerful approach to model the locations of spatially random helpers. It has been increasingly widely used for wireless network analysis. In [12], the methodologies of stochastic geometry were extensively reviewed in the context of wireless networks. In [25], different mobility models, such as the random waypoint model, were defined in terms of stochastic geometry. In [26, 27], the authors conducted a series of analysis on spatial and opportunistic ALOHA using stochastic geometry and various spatial performance measurements, including outage, throughput and transport. There have been some initial studies of cooperative wireless networks using stochastic geometry such as [28], [29] and [30]. In [28], four heuristic distributed uncoordinated relaying schemes were proposed for a two-hop time division multiple access (TDMA) based wireless system. In [29], the authors investigated three uncoordinated automatic repeat-request (ARQ) schemes, where single-helper diversity was considered in the first two schemes and no diversity was considered for the last local SNR-based scheme. In [30], a backoff timer-based scheme is designed and analyzed together with an energy-saving strategy for spatially

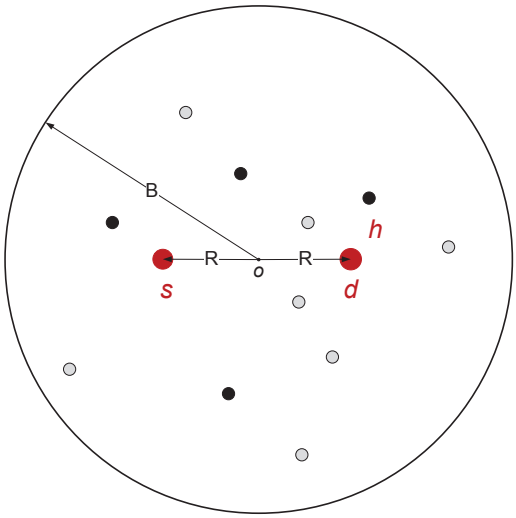

Fig. 1: System topology. Black nodes represent eligible helpers while gray ones are not helpers.

randomly distributed helpers. Although it only considers single-helper diversity, the proposed energy-saving strategy can selectively turn off certain helpers to significantly improve energy efficiency.

3. System Model

3.1. Channel Model

We consider a two-dimensional circle Borel area $\mathbb{B}(o, B)$ as shown in Fig. 1 with an origin o and radius B. The source node $s(-R, 0)$ and the destination node $d(0, R)$ are fixed, where $R < B$. A Rayleigh fading channel is considered between any data transmitter x and receiver y. The received instantaneous SNR, γ_{xy}, can be modelled by an exponential distribution [31] with a PDF conditional on the average SNR $\overline{\gamma}_{xy}$, given by

$$f_{\gamma_{xy}}(\gamma|\overline{\gamma}_{xy}) = \frac{1}{\overline{\gamma}_{xy}} e^{-\frac{\gamma}{\overline{\gamma}_{xy}}}, \qquad \gamma \geq 0. \tag{1}$$

Here, the PDF characteristic $\overline{\gamma}_{xy}$ depends on log-distance path loss, given by

$$\overline{\gamma}_{xy} = K_0 \|x - y\|^{-\alpha} \tag{2}$$

where $\|\cdot\|$ is the Euclidean distance operator, α is the path-loss exponent, and $K_0 = P_0/N_0$ is the ratio of transmit power to additive white Gaussian noise (AWGN) power. Specifically, when $\alpha = 2$, $\overline{\gamma}_{sd} = \frac{K_0}{4R^2}$. It should be noticed that, in a system with randomly distributed mobile helpers, $\overline{\gamma}_{xy}$ itself is a random variable depending on the locations of the nodes. Denoting the PDF of $\overline{\gamma}_{xy}$ by $f_{\overline{\gamma}_{xy}}(\gamma)$, we have the unconditional PDF of γ_{xy}, given by $f_{\gamma_{xy}}(\gamma|\overline{\gamma}_{xy})f_{\overline{\gamma}_{xy}}(\gamma)$.

3.2. Mobility Model and Poisson Point Process

We refer to all the nodes in $\mathbb{B}(o, B)$ except s and d as *potential helpers*. All the potential helpers are assumed subject to random direction (RD) mobility [10]. For the RD mobility model, a helper is uniformly placed at an initial position in $\mathbb{B}(o, B)$ at time $t = 0$ and then chooses a direction and a speed that are uniformly distributed, with a wrapping around assumption when it hits the boundary. According to [10], at any following time instant $t > 0$, the position of the helper preserves a uniform distribution. Thus, the location of a potential helper z in a polar coordination system, denoted by (r_{oz}, θ_z), follows the PDF expressed as

$$f_{r_{oz}}(r) = \frac{2r}{B^2}, \qquad 0 \le r \le B \tag{3}$$

$$f_{\theta_z}(\theta) = \frac{1}{2\pi}, \qquad 0 \le \theta \le 2\pi. \tag{4}$$

We further assume that the number of potential helpers in $\mathbb{B}(o, B)$, N_B, follows a Poisson distribution with a probability mass function (PMF):

$$\Pr\big[N_B = n\big] = \frac{{\lambda_B}^n}{n!} e^{-\lambda_B}, \qquad n = 0, 1, \ldots \tag{5}$$

where the intensity measure $\lambda_B = \lambda\pi B^2$ and λ is a constant. Combining the location distribution in (3)-(4) and the distribution of the number of potential helpers in (5), we see that the mobile potential helpers can be modeled by a homogeneous Poisson point process (PPP), denoted by Φ_B.

3.3. Distributed Cooperative Transmission

In this study, we consider a distributed cooperative transmission strategy. Whenever the source node s has a packet to transmit, it first sends a ready-

to-send (RTS) message and waits for a clear-to-send (CTS) response from the destination d. Based on the overheard RTS and CTS packets, a *potential helper* z can estimate the SNR between itself and s and d, denoted by γ_{sz} and γ_{zd}, respectively. Node z is automatically activated as a *helper* as long as $\gamma_{sz} \geq \Gamma_s$ and $\gamma_{zd} \geq \Gamma_d$. Here, Γ_s and Γ_d are thresholds pre-defined according to the quality-of-service (QoS) requirement. They can be the same constants for all potential helpers or vary with the actual locations of the potential helpers. For example, the potential helpers relatively far from s and d can use low thresholds to allow more nodes to participate in cooperative transmission.

Based on the above distributed helper selection, all helpers selected from Φ_B constitute a new point process defined by

$$\Phi_H = \left\{ z | z \in \Phi_B, \gamma_{sz} \geq \Gamma_s, \gamma_{zd} \geq \Gamma_d \right\}. \tag{6}$$

We show in Section 3.2 that the number of *potential helpers* in Φ_B and their locations are random variables. As a result of (6), the number of *helpers* (denoted by N) and their locations are also random variables for each cooperation. On receiving CTS, s transmits its data packet and the helpers that overhear the data packet successfully also relay the packet to d. Since multiple helpers may contribute to the relaying, we consider certain coordination schemes specified in Section 3.4 to minimize collisions among the helpers. Finally, d combines all the received signals based on MRC (to be discussed in Section 3.5). If the total SNR is above a decoding threshold γ_0, an ACK message is returned. Otherwise, the data transmission fails and s retransmits the packet after timeout or a $NACK$ message is received.

3.4. MAC for Multi-Helper Coordination

Due to the opportunistic behavior of the distributed helper selection described in Section 3.3, it is possible that multiple helpers are eligible for cooperative transmission. Thus, multiple helpers need to be properly coordinated with an effective MAC scheme to minimize collisions among their cooperative transmissions. We assume that the transmission channel is time-slotted and

each packet takes one time slot to transmit. An error-free broadcast feedback channel exists between d and all participating helpers, so that d returns an ACK or $NACK$ message after each transmission to indicate whether the relayed signal is successfully received or not. Based on the feedback, the helpers who have experienced collisions can schedule retransmission attempts according to certain MAC schemes. The above assumptions are typical for the analysis of cooperative MAC protocols [32, 33] and can be supported by simple techniques such as busy tone [34].

First, we consider an ALOHA-like MAC scheme for comparison purposes. If a packet from s is overheard by a potential helper z that satisfies $\gamma_{sz} \geq \Gamma_s$ and $\gamma_{zd} \geq \Gamma_d$ in one time slot, z becomes a helper and accesses the channel in the next slot with a probability p to forward this packet. If more than one helper transmits at the same time slot, a collision happens and the collided helpers reaccess the channel with the probability p in the next slot. A helper will remain silent once it has successfully occupied the channel for a transmission until all the helpers have made their cooperative contributions without collisions. After that, s starts to transmit a new packet.

In practice, the ALOHA scheme is not realistic since the delay increases exponentially with the number of participating helpers. Hence, we further propose a timer-based random backoff scheme, which adopts distributed coordination and perfectly complements the distributed cooperative transmission procedure in Section 3.3. As shown later in Section 4.4, the timer-based backoff scheme exhibits a good delay property.

Consider the circle area $\mathbb{B}(o, B)$ in Fig. 1. We divide this area into K rings as illustrated in Fig. 2. Each region M_i, $i = 1, ..., K$, is associated with a timer of a length $\Delta_i = i\delta$, where δ is a time constant. Take the example in Fig. 2. The helpers h_1 and h_2 in M_2 will relay their overheard signals after a backoff time 2δ, while the helper h_3 in M_3 will start its forwarding after a backoff time 3δ. Apparently, a collision will occur since there are two valid helpers in M_2 that transmit at the same time. When a collision happens a $NACK$ message is broadcast, so that not only the collided helpers but also the helpers who expect

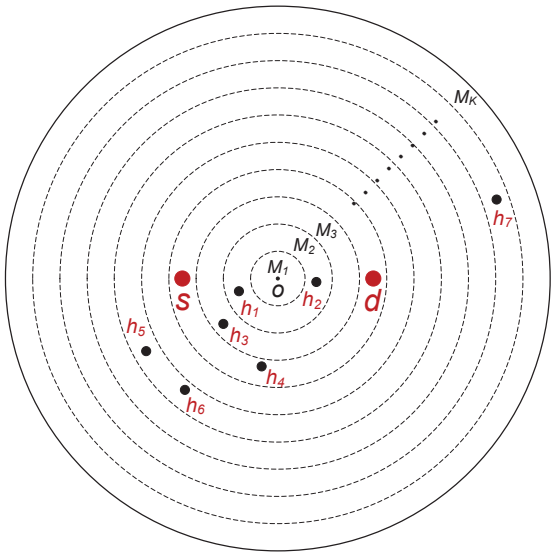

Fig. 2: Timer-based random backoff scheme.

to transmit after their backoff time are informed of the failed transmission. Similar to IEEE 802.11, the timer space of the region where the collided helpers are located is doubled, while the timers of the regions farther from the origin are deferred accordingly.

3.5. MRC and Upper Bound of Total SNR

Based on the distributed helper selection in Section 3.3, some potential helpers become active helpers and they are coordinated with the MAC schemes in Section 3.4 and relay their overheard signals using an AF scheme [13, 8]. At the destination node d, all the received signals are combined with MRC and the total SNR is given by [13]

$$\gamma_{tot} = \gamma_{sd} + \sum_{i=1}^{N} \frac{\gamma_{si}\gamma_{id}}{\gamma_{si} + \gamma_{id} + 1} \tag{7}$$

where the number of helpers (N), the SNR between s, d, and each helper i (γ_{sd}, γ_{si}, and γ_{id}), are all random variables, which depend on the topology defined in Section 3.1.

In practice, because (7) is often not tractable, the upper bound of (7) can be used instead. An upper bound of γ_{tot} is proposed in [14, 15], given by

$$\gamma_{ub} = \gamma_{sd} + \sum_{i=1}^{N} \gamma_i \tag{8}$$

where $\gamma_i = \min(\gamma_{si}, \gamma_{id})$. It is worth mentioning that a lower bound can be formulated by defining $\gamma_i = \min(\gamma_{si}, \gamma_{id})/2$ [14]. According to (1), it is easy to show that γ_i also follows an exponential distribution with a PDF

$$f_{\gamma_i}(\gamma|\tau_i) = \frac{1}{\tau_i} e^{-\frac{\gamma}{\tau_i}}, \qquad \gamma \geq 0 \tag{9}$$

where

$$\tau_i = \frac{\overline{\gamma}_{si}\overline{\gamma}_{id}}{\overline{\gamma}_{si} + \overline{\gamma}_{id}}. \tag{10}$$

In [8], the non-i.i.d. PDF of γ_{ub} conditional on $\tau_1, \ldots, \tau_N$ is obtained as

$$f_{\gamma_{ub}}(\gamma|\tau_1, \tau_2, \ldots, \tau_N) = \frac{\beta_0}{\overline{\gamma}_{sd}} e^{-\frac{\gamma}{\overline{\gamma}_{sd}}} + \sum_{i=1}^{N} \frac{\beta_i}{\tau_i} e^{-\frac{\gamma}{\tau_i}} \tag{11}$$

where

$$\beta_0 = \prod_{i=1}^{N} \left(1 - \frac{\tau_i}{\overline{\gamma}_{sd}}\right)^{-1}$$

$$\beta_i = \left(1 - \frac{\overline{\gamma}_{sd}}{\tau_i}\right)^{-1} \prod_{k=1, k\neq i}^{N} \left(1 - \frac{\tau_k}{\tau_i}\right)^{-1}, \quad i = 1, \ldots, N.$$

4. Unconditional Success Probability and Delay

In this section, we first derive the distribution of the number of helpers (N) in the random set defined in (6). Then, we obtain the PDF of the locations of the random helpers. After that, the unconditional counterpart of (11) is obtained for a given number of helpers n. Two simplified approximations are also proposed for the unconditional PDF of the SNR upper bound. Based on these preparation steps, we eventually provide the analysis for the unconditional success probability, which is the complement of the unconditional outage probability. At the end, we analyze the delay involved with different MAC schemes and evaluate the outage-delay tradeoff.

4.1. Exact Form of Unconditional PDF of SNR Upper Bound

For any potential helper z in Φ_B, its SNR of the channel from s to z and the SNR of the channel from z to d (i.e., γ_{sz} and γ_{zd}) are independent. According to (1), (2) and (6), the probability that a potential helper z is an eligible helper can be written as

$$\begin{aligned} P_z &= \Pr\big[\gamma_{sz} \geq \Gamma_s, \gamma_{zd} \geq \Gamma_d\big] \\ &= \int_{\Gamma_s}^{\infty} \int_{\Gamma_d}^{\infty} f_{\gamma_{sz}}(\gamma_1|\overline{\gamma}_{sz}) f_{\gamma_{zd}}(\gamma_2|\overline{\gamma}_{zd})\, \mathrm{d}\gamma_1\, \mathrm{d}\gamma_2 \\ &= \exp\Big(\frac{-\Gamma_s\|s-z\|^{\alpha} - \Gamma_d\|z-d\|^{\alpha}}{K_0}\Big). \end{aligned} \tag{12}$$

As seen in (12), whether a node is an eligible helper or not is related to its location. Thus, the helper set Φ_H can be generated from Φ_B by retaining z in Φ_B with a probability P_z and deleting it with a probability $(1 - P_z)$. The resulting point process of remaining nodes forms Φ_H. This is actually the result of an independent $p(x)$-thinning operation to Φ_B. The $p(x)$-thinning operation defines a retention probability $p(x)$ for each point x of a PPP and yields a thinned point process by deleting the point x with a probability $1 - p(x)$ [11]. According to *Prekopa's Theorem* [11], the number of eligible helpers is still Poisson distributed with a parameter λ_H, given by

$$\lambda_H = \int_0^{B} \int_0^{2\pi} \exp\Big(\frac{-\Gamma_s\|s-z\|^{\alpha} - \Gamma_d\|z-d\|^{\alpha}}{K_0}\Big) \frac{\lambda_B}{\pi B^2}\, r\, \mathrm{d}r\, \mathrm{d}\theta. \tag{13}$$

In this study, we consider the following location-dependant thresholds for helper selection:

$$\Gamma_s = \Gamma_d = \frac{K_0 \ln(2r_{oz})}{2(r_{oz}^2 + R^2)} \tag{14}$$

where r_{oz} is the distance between a potential helper z and the origin and $\ln(\cdot)$ is the natural logarithm. As such, when $\alpha = 2$, we have

$$\lambda_H = \frac{\lambda_B}{B}. \tag{15}$$

Thus, the number of helpers in Φ_H is Poisson distributed with the PMF

$$\Pr\big[N = n\big] = \frac{{\lambda_H}^n}{n!} e^{-\lambda_H}, \qquad n = 0, 1, \ldots \tag{16}$$

Proposition 1. *For a given $N = n$, when the selection thresholds are defined in (14) and $\alpha = 2$, the distance between a helper in Φ_H and the origin (denoted by r_{oh}) follows a uniform distribution with the normalized PDF:*

$$f_{r_{oh}}(r) = \frac{1}{B}, \qquad 0 \le r \le B. \tag{17}$$

Proof. Here, r_{oz} denotes the distance between a potential helper z and the origin o, while r_{oh} is the distance between an eligible helper h and the origin. Based on the relationship of r_{oz} and r_{oh}, we can obtain

$$\begin{aligned} \Pr[r_{oh} \le r] &= \Pr\big[r_{oz} \le r \text{ and } z \text{ is selected as } h | r_{oz}\big] \\ &= \int_0^r f_{r_{oz}}(x) P_z(x)\, \mathrm{d}x. \end{aligned} \tag{18}$$

Substituting $f_{r_{oz}}$ and P_z in (18) by (3) and (12), respectively, we can easily prove (17). □

Proposition 2. *When $\alpha = 2$ and the thresholds of helper selection are defined as(14), any random variable τ_i in (10) has a PDF given by*

$$f_\tau(t) = \frac{K_0}{4Bt^2}\Big(\frac{K_0}{2t} - R^2\Big)^{-\frac{1}{2}}, \qquad \frac{K_0}{2(B^2+R^2)} < t < \frac{K_0}{2R^2}. \tag{19}$$

Proof. According to Apollonius' theorem, we combine (2) and (10) and have

$$\begin{aligned} \frac{1}{\tau_i} &= \frac{\parallel s - h \parallel^2 + \parallel h - d \parallel^2}{K_0} \\ &= 2(r_{oh}^2 + R^2)/K_0 \end{aligned} \tag{20}$$

where r_{oh} is the distance of any helper h in Φ_H to the origin o. From Proposition 1, we know that r_{oh} follows a uniform distribution. Based on (17) and (20), it is straightforward to obtain (19) for the PDF of any τ_i. □

Applying the PDF of τ_i, we can remove the conditions of $\tau_1, \ldots, \tau_N$ in (11). The unconditional PDF of the upper bound of total SNR when $N = n$ can be expressed as

$$f_{\gamma_{ub}}(\gamma) = \underbrace{\int \cdots \int}_{n} f_{\gamma_{ub}}(\gamma | t_1, t_2, \cdots, t_n) \cdot f_{\tau_1}(t_1) \cdots f_{\tau_n}(t_n)\, \mathrm{d}t_1 \cdots \mathrm{d}t_n. \tag{21}$$

Lemma 1. *For a given $N = n$, the exact form of the unconditional PDF of γ_{ub} is expressed as*

$$f_{\gamma_{ub}}(\gamma) = \underbrace{\frac{C^n}{\overline{\gamma}_{sd}} e^{-\frac{\gamma}{\overline{\gamma}_{sd}}}}_{F_1} + \underbrace{n \int_{\mathbb{I}} W(\gamma, t) U(t)^{n-1} \, \mathrm{d}t}_{F_2} \tag{22}$$

where $\mathbb{I}$ is the interval $\left(\frac{K_0}{2(B^2+R^2)}, \frac{K_0}{2R^2}\right)$ and

$$\begin{aligned} C &= 1 + \frac{R}{B} \ln\left(\frac{B-R}{B+R}\right) \\ W(\gamma, t) &= \frac{e^{-\frac{\gamma}{t}}}{t - \overline{\gamma}_{sd}} f_\tau(t) \\ U(t) &= 1 + \frac{K_0}{4B\sqrt{tY}} \ln\left(\frac{Bt - \sqrt{tY}}{Bt + \sqrt{tY}}\right), \quad Y = \frac{K_0}{2} - R^2 t. \end{aligned}$$

Proof. The proof of Lemma 1 is given in Appendix A. □

4.2. Two Approximation Forms of Unconditional PDF of SNR Upper Bound

In (22), F_2 is very complicated and a closed-form expression is not tractable. Besides, the exact form does not shed much insight on deriving the success or outage probability. Hence, we propose to use the Newton-Cotes formula [35] of the open type to approximate (22). Specifically, redefining the integral interval $\mathbb{I} = \left(\frac{K_0}{2(B^2+R^2)}, \frac{K_0}{2R^2}\right)$ as (a, b), we have the i^{th} Newton-Cotes sampling point of m degree as $x_{mi} = a + \frac{i(b-a)}{m}$. Then, (22) can be approximated by

$$f_{\gamma_{ub}}(\gamma) \approx \frac{C^n}{\overline{\gamma}_{sd}} e^{-\frac{\gamma}{\overline{\gamma}_{sd}}} + n \sum_{i=1}^{m-1} A_{mi} W(\gamma, x_{mi}) U(x_{mi})^{n-1} \tag{23}$$

where A_{mi} is the i^{th} coefficient of the Newton-Cotes formula of m degree. When $B \gg R$, it is obvious that $C \approx 1$ and $U(t) \approx 1$. As a result, (23) can be further simplified as

$$f_{\gamma_{ub}}(\gamma) \approx \frac{1}{\overline{\gamma}_{sd}} e^{-\frac{\gamma}{\overline{\gamma}_{sd}}} + n \sum_{i=1}^{m-1} A_{mi} W(\gamma, x_{mi}). \tag{24}$$

4.3. Approximation of Unconditional Success Probability

The success probability, which is the complement of the outage probability, is defined as the probability that γ_{ub} is above a certain threshold γ_0 when $N = n$,

which can be expressed as

$$P_s(n) = \int_{\gamma_0}^{\infty} f_{\gamma_{ub}}(\gamma)\, d\gamma. \tag{25}$$

Lemma 2. *For a given $N = n$, the success probability of the cooperative wireless system as described in Section 3.1 can be approximated by*

$$P_s(n) \approx C^n e^{-\frac{\gamma_0}{\overline{\gamma}_{sd}}} + n \sum_{i=1}^{m-1} x_{mi} A_{mi} W(\gamma_0, x_{mi}) U(x_{mi})^{n-1} \tag{26}$$

where x_{mi} and A_{mi} are the i^{th} Newton-Cotes sampling point and coefficient of m degree, respectively. If $B \gg R$, (26) can be further simplified as

$$P_s(n) \approx E + nA \tag{27}$$

where E and A are constants given by

$$E = e^{-\frac{\gamma_0}{\overline{\gamma}_{sd}}} \tag{28}$$

$$A = \sum_{i=1}^{m-1} x_{mi} A_{mi} W(\gamma_0, x_{mi}). \tag{29}$$

Proof. It can be easily proved that $W(\gamma, t)$ satisfies the following property

$$\int_{\gamma_0}^{\infty} W(\gamma, t) \mathrm{d}\gamma = tW(\gamma_0, t). \tag{30}$$

Applying this property to (23) and (25), we have

$$\begin{aligned} P_s(n) &\approx \int_{\gamma_0}^{\infty} \frac{C^n}{\overline{\gamma}_{sd}} e^{-\frac{\gamma}{\overline{\gamma}_{sd}}}\, d\gamma + n \sum_{i=1}^{m-1} A_{mi} U(x_{mi})^{n-1} \int_{\gamma_0}^{\infty} W(\gamma, x_{mi})\, d\gamma \\ &= C^n e^{-\frac{\gamma_0}{\overline{\gamma}_{sd}}} + n \sum_{i=1}^{m-1} A_{mi} U(x_{mi})^{n-1} \cdot x_{mi} W(\gamma_0, x_{mi}) \\ &= C^n e^{-\frac{\gamma_0}{\overline{\gamma}_{sd}}} + n \sum_{i=1}^{m-1} x_{mi} A_{mi} W(\gamma_0, x_{mi}) U(x_{mi})^{n-1}. \end{aligned}$$

Thus, (26) is proved. Similarly, (27) can be derived by using the property in (30) to (24) and (25). □

Theorem 1. *The unconditional success probability of the wireless diversity system that uses the distributed cooperative transmission with spatially random helpers as described in Section 3.1 is given by*

$$\mathcal{P}_s = \sum_{i=1}^{\infty} \frac{{\lambda_H}^n}{n!} e^{-\lambda_H} P_s(n). \tag{31}$$

When $\alpha = 2$ and $B \gg R$, (31) can be approximated by

$$\mathcal{P}_s \approx E + \lambda_H A \tag{32}$$

where λ_H is the intensity measure of Φ_H given in (13), and E and A are constants given in (28) and (29), respectively.

Proof. Eq. (31) provides the unconditional expectation of the success probability. It can be easily obtained by averaging $P_s(n)$ with the PMF of N, which follows the Poisson distribution in (16). Eq. (32) is a straightforward result of (27) and (31), since the mean of N is equal to the intensity λ_H. □

4.4. Delay Analysis of MAC Coordination Schemes

As discussed in Section 3.4, we consider both an ALOHA-like MAC scheme and a timer-based random backoff scheme to coordinate multiple available helpers. These MAC schemes may introduce different levels of collisions, which have a direct impact on the cooperative transmission. In this section, we analyze the delay of the two MAC schemes, which is another important performance metric in addition to the success probability evaluated in Section 4.3.

In the ALOHA-like MAC scheme, an eligible helper accesses the channel with a probability p to forward the overheard packet. Given n eligible helpers in total, if i ($1 \le i \le n$) helpers have not made their relaying contributions, the probability that the channel is successfully occupied by only one of these helpers is given by

$$P_a(i) = \binom{i}{1} p(1-p)^{i-1}, \quad i = 1, \ldots, n. \tag{33}$$

Let L denote the number of wasted time slots before a slot is successfully occupied by one of the i helpers. Obviously, L follows a geometric distribution with

the parameter $P_a(i)$ and has a PMF

$$\Pr\big[L = l|i\big] = \big[1 - P_a(i)\big]^{l-1} P_a(i), \quad l = 1, 2, \ldots \tag{34}$$

Thus, the average number of time slots before one of the i helpers successfully captures the channel and relays the packet is given by

$$\overline{L}(i) = \frac{1}{P_a(i)}.$$

The same contention process repeats until each of the n helpers has successfully occupied the channel and relayed the packet. Therefore, we can obtain the total delay as

$$D_A(n) = \sum_{i=1}^{n} \frac{\xi}{ip(1-p)^{i-1}} \tag{35}$$

where ξ is the time slot for a packet transmission.

As shown later in Section 5, $D_A(n)$ increases exponentially with n. To simplify the calculation in (35), we can approximate the delay by

$$\tilde{D}_A(n) = \varepsilon \zeta^n \tag{36}$$

where the coefficients ε and ζ can be determined by fitting two sample values $D_A(1)$ and $D_A(\tilde{n})$ with (36). Thus, we have

$$\varepsilon = D_A(1), \qquad \zeta = \left[\frac{D_A(\tilde{n})}{D_A(1)}\right]^{\frac{1}{\tilde{n}}}. \tag{37}$$

Combining (16) and (35), we further obtain the average delay with the ALOHA scheme as

$$\overline{D}_A = \sum_{i=1}^{\infty} \frac{{\lambda_H}^n}{n!} e^{-\lambda_H} \tilde{D}_A(n) = \varepsilon e^{\lambda_H(\zeta - 1)}. \tag{38}$$

For the timer-based backoff scheme, it is intractable to derive a closed-form expression for the delay. Therefore, we provide a numerical approximation based on the observation of the simulation results. In particular, the delay of the timer-based backoff scheme is approximated by

$$\tilde{D}_T(n) = \mu_2 n^2 + \mu_1 n + \mu_0 \tag{39}$$

where the coefficients μ_2, μ_1, and μ_0 can be obtained by using three delay sample values when the number of helpers is 1, $\frac{\tilde{n}}{2}$, and $\tilde{n}$, which are denoted by $D_T(1)$, $D_T(\frac{\tilde{n}}{2})$, and $D_T(\tilde{n})$, respectively. Then, based on the Lagrange numerical analytical expression [36], we have

$$\mu_2 = \frac{D_T(1)}{(1-\tilde{n}/2)(1-\tilde{n})} - \frac{D_T(\frac{\tilde{n}}{2})}{(\tilde{n}/2-1)\tilde{n}/2} + \frac{D_T(\tilde{n})}{(\tilde{n}-1)\tilde{n}/2} \tag{40}$$

$$\mu_1 = -\frac{(3\tilde{n}/2)D_T(1)}{(1-\tilde{n}/2)(1-\tilde{n})} + \frac{(1+\tilde{n})D_T(\frac{\tilde{n}}{2})}{(\tilde{n}/2-1)\tilde{n}/2} - \frac{(1+\tilde{n}/2)D_T(\tilde{n})}{(\tilde{n}-1)\tilde{n}/2} \tag{41}$$

$$\mu_0 = \frac{\tilde{n}^2 D_T(1)}{2(1-\tilde{n}/2)(1-\tilde{n})} - \frac{\tilde{n}D_T(\frac{\tilde{n}}{2})}{(\tilde{n}/2-1)\tilde{n}/2} + \frac{\tilde{n}D_T(\tilde{n})}{2(\tilde{n}-1)\tilde{n}/2}. \tag{42}$$

We further combine (16) and (39) to evaluate the average delay of the timer-based backoff scheme by

$$\overline{\mathcal{D}}_T = \sum_{i=1}^{\infty} \frac{{\lambda_H}^n}{n!} e^{-\lambda_H} \tilde{D}_T(n) = \mu_2 \lambda_H^2 + (\mu_2 + \mu_1)\lambda_H + \mu_0. \tag{43}$$

4.5. Outage-Delay Tradeoff

As the complement of success probability, the outage probability, denoted by $\mathcal{P}_o$, is the probability that the total SNR at d falls below the decoding threshold γ_0, which means that a data transmission fails. When the direct channel between s and d is poor, more helpers should be involved for a higher diversity gain. On the other hand, a larger overhead of coordination delay may also be introduced due to collisions among more helpers. As seen, there is a tradeoff between the outage probability and the delay.

In Section 4.3, the success probability $\mathcal{P}_s$ is derived and given in (32). Hence, the outage probability can be written as $\mathcal{P}_o = 1 - \mathcal{P}_s$. The delay of the two MAC schemes is analyzed in Section 4.4 and given in (38) and (43). For the ALOHA-like scheme, we can relate the delay to the outage probability as follows:

$$\overline{\mathcal{D}}_A = \varepsilon \exp\Big(\frac{1-E-\mathcal{P}_o}{A}(\zeta - 1)\Big). \tag{44}$$

According to (32), we have $\lambda_H = \frac{1-E-\mathcal{P}_o}{A}$, which can be applied to (38) to obtain (44). Similarly, the outage-delay tradeoff for the timer-based backoff

scheme can be expressed as

$$\overline{\mathcal{D}}_T = \mu_2\Big(\frac{1-E-\mathcal{P}_o}{A}\Big)^2 + (\mu_2+\mu_1)\Big(\frac{1-E-\mathcal{P}_o}{A}\Big) + \mu_0. \tag{45}$$

Considering the overall system performance, we are interested in the ratio of the success probability to the delay, defined by

$$\mathcal{B} = \frac{\mathcal{P}_s}{\mathcal{D}} \tag{46}$$

in which the delay $\mathcal{D}$ can be interpreted as the price paid to achieve certain success probability $\mathcal{P}_s$. When the ALOHA scheme is used, based on (32) and (38), the success/delay ratio is written as

$$\mathcal{B}_A = \frac{E+\lambda_H A}{\varepsilon e^{\lambda_H(\zeta-1)}}. \tag{47}$$

Taking the first-order derivative of (47) with respect to λ_H, we can find that the success/delay ratio is maximized when

$$\lambda_H = \hat{\lambda}_A = \frac{1}{\zeta-1} - \frac{E}{A}. \tag{48}$$

Likewise, for the timer-based backoff scheme, the success/delay ratio can be obtained from (32) and (43) as

$$\mathcal{B}_T = \frac{E+\lambda_H A}{\mu_2\lambda_H^2 + (\mu_2+\mu_1)\lambda_H + \mu_0}. \tag{49}$$

Similarly, the success/delay ratio is maximized when

$$\lambda_H = \hat{\lambda}_T = \frac{-\mu_2 E + \sqrt{(\mu_2 E)^2 + \mu_2\mu_0 A^2 - \mu_2(\mu_1+\mu_2)AE}}{\mu_2 A}. \tag{50}$$

5. Numerical and Simulation Results

In this section, we first validate the accuracy of the linear approximation of Lemma 2. Then, we compare the numerical results and simulation results for the unconditional success probability $\mathcal{P}_s$ derived in Theorem 1 and the delay of the ALOHA scheme and the backoff timer-based scheme, $\overline{\mathcal{D}}_A$ and $\overline{\mathcal{D}}_T$, given in (38) and (43). Finally, we present numerical results demonstrating the outage-delay tradeoff. The main system parameters are given in Table 1.

Table 1: System parameters.

Definition	**Symbol**	**Value**
Intensity measure of Φ_B	λ_B	500
Location parameter of nodes s and d	R	5
Circle area radius	B	40
Transmit SNR	K_0	14.7 dB
Decoding SNR threshold	γ_0	$2\overline{\gamma}_{sd}$
Path loss exponent	α	2
ALOHA channel access probability	p	0.4
Number of contention regions	K	10
Time slot length	ξ	1

5.1. Analysis Validation

Fig. 3(a) shows how the success probability $P_s(n)$ varies with the number of helpers n. As seen, the simulation results exhibit an apparent linear tendency and our analysis results have a good approximation accuracy. Fig. 3(a) further shows the analysis error versus the approximation degree m. As expected, the higher the degree m, the closer the approximation. For example, when $m = 6$, the relative error is as low as 4%.

Fig. 3(b) compares the numerical results and simulation results to verify the conclusion in Theorem 1. If the nodes are located according to the system model in Section 3.2 and the helpers are selected by the distributed algorithm in Section 3.3, the number of helpers follows a Poisson distribution of a parameter λ_H. It is clearly shown in Fig. 3(b) that the unconditional success probability varies linearly with λ_H, which confirms Eq. (32).

Fig. 4(a) shows the numerical and simulation results of delay with the ALOHA scheme and the timer-based backoff scheme. As seen, the simulation results match well the numerical approximations in (36) and (39). Here, the coefficients of the delay approximation for the ALOHA scheme are $\varepsilon = 2.50$ and $\zeta = 1.44$, given that the access probability $p = 0.4$. In this case, the de-

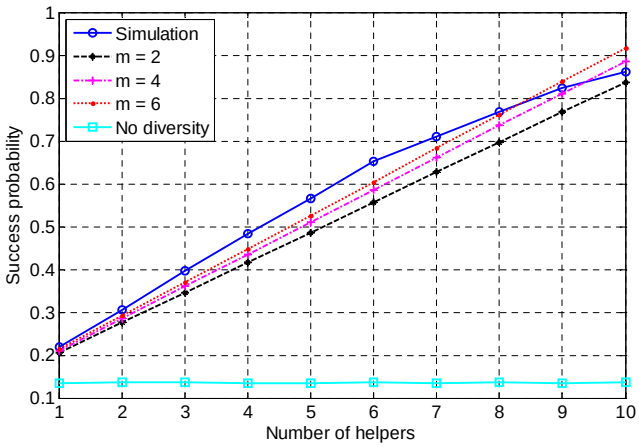

(a) Success probability vs. the number of helpers.

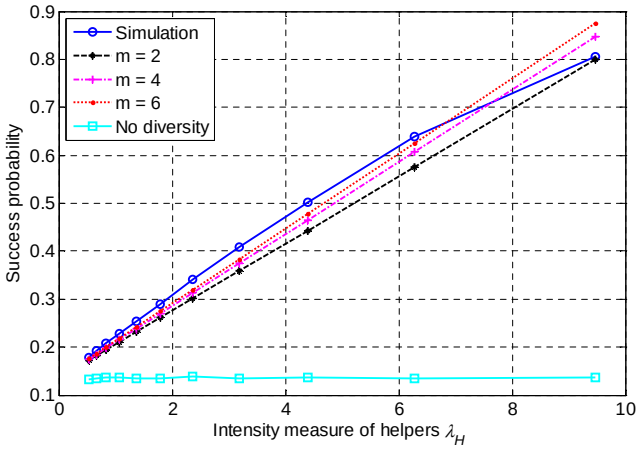

(b) Success probability vs. the intensity measure λ_H.

Fig. 3: Success probability.

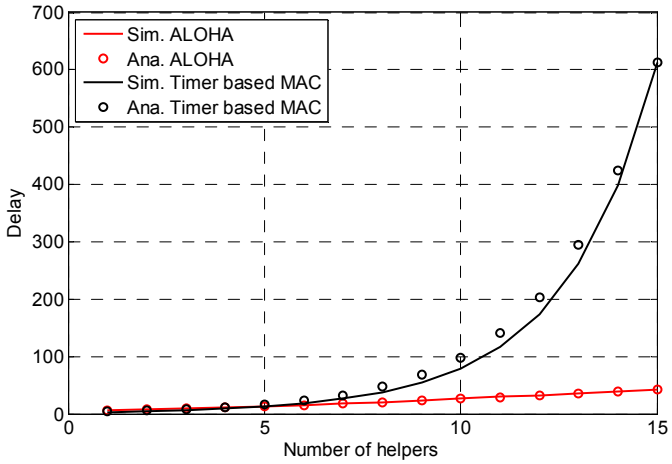

(a) Delay vs. the number of helpers.

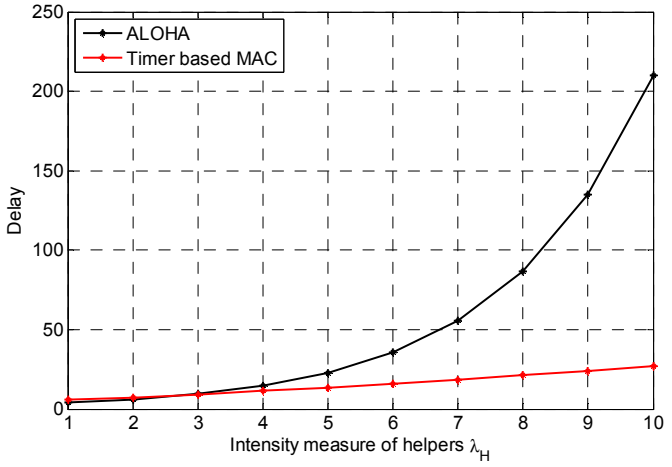

(b) Delay vs. the intensity measure λ_H.

Fig. 4: Delay performance.

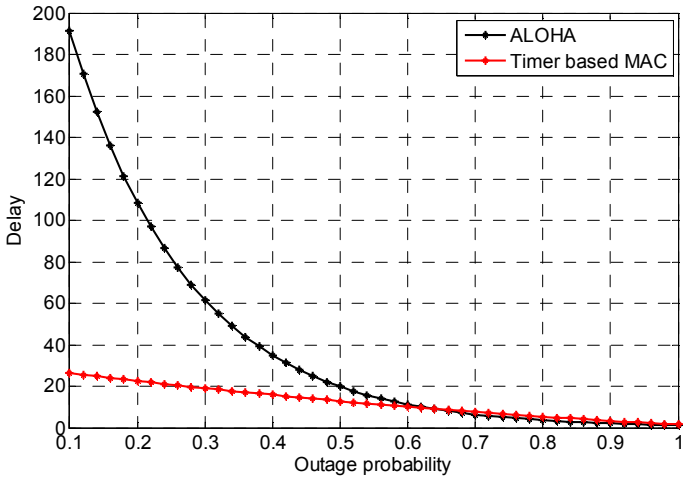

Fig. 5: Outage-delay tradeoff ($m = 6$).

lay increases exponentially with the number of helpers due to collisions. On the other hand, for the timer-based backoff scheme, we choose the parameter $\tilde{n} = 15$ and determine the coefficients of the delay approximation as $\mu_2 = 0.075$, $\mu_1 = 1.46$, and $\mu_0 = 3.98$. Apparently, the timer-based backoff scheme performs much better in terms of delay when the number of helpers are potentially large. This observation is also verified by Fig. 4(b), which shows the numerical results of (38) and (43). It is seen that when the nodes are densely deployed with a large λ_H, the timer-based backoff scheme is more effective in handling collisions and mitigating the delay overhead.

5.2. Outage-Delay Tradeoff

While the success probability presents a linear increase with the number of helpers, the delay also increases fast due to the multi-helper coordination. Fig. 5 shows the numerical results of (44) and (45), which demonstrates the tradeoff between the outage probability and the delay. As observed in Fig. 5, when the QoS requirement of the outage probability is very low, there is a much larger delay overhead with the ALOHA scheme compared to the timer-based backoff scheme. As the outage requirement is further relaxed, the difference between these two MAC schemes diminishes.

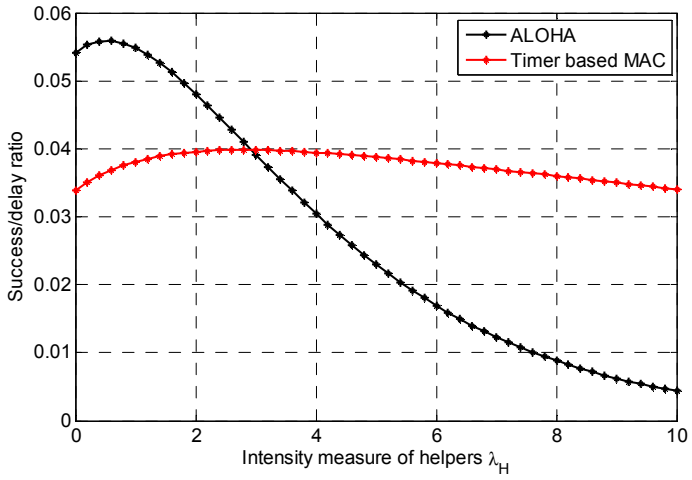

Fig. 6: Success/delay ratio vs. the intensity measure λ_H.

Fig. 6 shows the variation of the success/delay ratio defined in (47) and (49) with the intensity measure λ_H. This success/delay ratio can be interpreted as the price paid in terms of delay to achieve certain required success probability. As seen, the success/delay ratio of the ALOHA scheme drops dramatically after the ratio reaches the maximum when the helper intensity measure $\lambda_H = \hat{\lambda}_A = 0.69$, which is obtained from (48). In contrast, the timer-based backoff scheme experiences much smaller fluctuation. The success/delay ratio is maximal when $\lambda_H = \hat{\lambda}_T = 2.8$ as calculated by (50). It means that the timer-based backoff scheme also performs well in a dense network. Since the intensity measure of helpers λ_H is related to that of potential helpers λ_B according to (15), we can use pre-selection to adapt λ_H so that the success/delay ratio is maximized.

6. Conclusions and Future Work

In this paper, we considered a wireless diversity system with multiple mobile helpers using a distributed cooperation strategy. As the helpers are assumed to be randomly deployed in certain area, the number of helpers and their spatial locations are not deterministic or known in advance. Taking into account the spatial random characteristics of helpers, we analyzed the cooperative transmis-

sion success probability. We found that the success probability is linear with the number of helpers when the system covers a sufficiently large area. Further, because the number of eligible helpers is random itself, the unconditional success probability is only related to the intensity measure of the point process of helpers. Considering an ALOHA-like MAC scheme and a timer-based random backoff scheme, we quantified the tradeoff between the success probability and delay, and defined the performance metric success/delay ratio. The ratio can be maximized by adapting the helper intensity λ_H which is linearly related to the overall node intensity λ_B.

The conclusions and analysis results of this study are not only mathematically proved but also validated by simulations. The approximations of the success probability simplify the performance evaluation and exhibit a high accuracy. This work also builds a basic framework to analyze wireless diversity systems with distributed cooperation. Exploiting the mobility models defined with stochastic geometry, we can naturally involve more mobility patterns of nodes in the analysis. The analytical approach can be extended to consider a node topology other than a Poisson point process. Moreover, different helper selection strategies can be investigated by adjusting the thinning process accordingly to generate the helper set.

Appendix A. Proof of Lamma 1

Proof. The original expression of the unconditional PDF of γ_{ub} is given in (21). Based on (11), (21) can be divided into the following two parts:

$$F_1 = \underbrace{\int_{\mathbb{I}} \cdots \int_{\mathbb{I}}}_{n} \frac{\beta_0}{\overline{\gamma}_{sd}} e^{-\frac{\gamma}{\overline{\gamma}_{sd}}} f_{\tau_1}(t_1) \cdots f_{\tau_n}(t_n) \, \mathrm{d}t_1 \cdots \mathrm{d}t_n \tag{51}$$

$$F_2 = \underbrace{\int_{\mathbb{I}} \cdots \int_{\mathbb{I}}}_{n} \sum_{i=1}^{n} \frac{\beta_i}{t_i} e^{-\frac{\gamma}{t_i}} f_{\tau_1}(t_1) \cdots f_{\tau_n}(t_n) \, \mathrm{d}t_1 \cdots \mathrm{d}t_n. \tag{52}$$

For F_1, since τ_i $(i = 1, \cdots, n)$ are independent of each other, and $e^{-\frac{\gamma}{\overline{\gamma}_{sd}}}$ is

separable from β_0 and $f_\tau(t_i)$, we rewrite (51) as

$$F_1 = \frac{1}{\overline{\gamma}_{sd}} e^{-\frac{\gamma}{\overline{\gamma}_{sd}}} \left[\int_{\mathbb{I}} \left(1 - \frac{t}{\overline{\gamma}_{sd}}\right)^{-1} f_\tau(t)\, \mathrm{d}t \right]^n = \frac{C^n}{\overline{\gamma}_{sd}} e^{-\frac{\gamma}{\overline{\gamma}_{sd}}}$$

where

$$C = \int_{\mathbb{I}} \left(1 - \frac{t}{\overline{\gamma}_{sd}}\right)^{-1} f_\tau(t)\, \mathrm{d}t = 1 + \frac{R}{B} \ln\left(\frac{B-R}{B+R}\right).$$

Since $t_1 \cdots t_n$ are symmetric for the integral in (52), the following equation holds for any $i \neq j$:

$$\underbrace{\int_{\mathbb{I}} \cdots \int_{\mathbb{I}}}_{n} \frac{\beta_i}{t_i} e^{-\frac{\gamma}{t_i}} f_{\tau_1}(t_1) \cdots f_{\tau_n}(t_n) \mathrm{d}t_1 \cdots \mathrm{d}t_n = \underbrace{\int_{\mathbb{I}} \cdots \int_{\mathbb{I}}}_{n} \frac{\beta_j}{t_j} e^{-\frac{\gamma}{t_j}} f_{\tau_1}(t_1) \cdots f_{\tau_n}(t_n) \mathrm{d}t_1 \cdots \mathrm{d}t_n.$$

Thus, (52) can be derived as follows:

$$\begin{aligned}
F_2 &= \underbrace{\int_{\mathbb{I}} \cdots \int_{\mathbb{I}}}_{n} \sum_{i=1}^{n} \frac{\beta_i}{t_i} e^{-\frac{\gamma}{t_i}} f_{\tau_1}(t_1) \cdots f_{\tau_n}(t_n)\, \mathrm{d}t_1 \cdots \mathrm{d}t_n \\
&= \sum_{i=1}^{n} \underbrace{\int_{\mathbb{I}} \cdots \int_{\mathbb{I}}}_{n} \frac{\beta_i}{t_i} e^{-\frac{\gamma}{t_i}} f_{\tau_1}(t_1) \cdots f_{\tau_n}(t_n)\, \mathrm{d}t_1 \cdots \mathrm{d}t_n \\
&= n \underbrace{\int_{\mathbb{I}} \cdots \int_{\mathbb{I}}}_{n} \frac{\beta_1}{t_1} e^{-\frac{\gamma}{t_1}} f_{\tau_1}(t_1) \cdots f_{\tau_n}(t_n)\, \mathrm{d}t_1 \cdots \mathrm{d}t_n.
\end{aligned}$$

It is further noticed that, the above integral has two separate parts which depend on either t_1 or t_i $(i = 2, \ldots, n)$. Therefore, replacing t_1 by t and t_i $(i = 2, \ldots, n)$ by s and considering τ_i $(i = 2, \ldots, n)$ are independent of each other, we can simplify (53) as follows:

$$\begin{aligned}
F_2 &= n \underbrace{\int_{\mathbb{I}} \cdots \int_{\mathbb{I}}}_{n} \frac{\beta_1}{t_1} e^{-\frac{\gamma}{t_1}} f_{\tau_1}(t_1) \cdots f_{\tau_n}(t_n)\, \mathrm{d}t_1 \cdots \mathrm{d}t_n \\
&= n \int_{\mathbb{I}} \frac{e^{-\frac{\gamma}{t}}}{t - \overline{\gamma}_{sd}} f_\tau(t) \left[\int_{\mathbb{I}} \left(1 - \frac{s}{t}\right)^{-1} f_\tau(s) \mathrm{d}s \right]^{n-1} \mathrm{d}t \\
&= n \int_{\mathbb{I}} W(\gamma, t) U(t)^{n-1}\, \mathrm{d}t
\end{aligned}$$

where we define

$$W(\gamma, t) \triangleq \frac{e^{-\frac{\gamma}{t}}}{t - \overline{\gamma}_{sd}} f_\tau(t)$$

$$U(t) \triangleq \int_{\mathbb{I}} \left(1 - \frac{s}{t}\right)^{-1} f_\tau(s)\, \mathrm{d}s = 1 + \frac{K_0}{4B\sqrt{tY}} \ln\left(\frac{Bt - \sqrt{tY}}{Bt + \sqrt{tY}}\right)$$

and $Y \triangleq \frac{K_0}{2} - R^2 t$. Thus, Lemma 1 is proved. □

References

[1] A. Sendonaris, E. Erkip, B. Aazhang, User cooperation diversity–Part I: System description, IEEE Trans. Commun. 51 (11) (2003) 1927–1938.

[2] A. Sendonaris, E. Erkip, B. Aazhang, User cooperation diversity–Part II: Implementation aspects and performance analysis, IEEE Trans. Commun. 51 (11) (2003) 1939–1948.

[3] H. Tarng, B. Chuang, P. Liu, A relay node deployment method for disconnected wireless sensor networks: Applied in indoor environments, Journal of Network and Computer Applications 32 (3) (2009) 652–659.

[4] D. S. Kumar, N. Nagarajan, Relay technologies and technical issues in IEEE 802.16j mobile multi-hop relay (MMR) networks, Journal of Network and Computer Applications 36 (1) (2013) 91–102.

[5] S. Al-Sultan, M. M. Al-Doori, A. H. Al-Bayatti, H. Zedan, A comprehensive survey on vehicular ad hoc network, Journal of Network and Computer Applications 37 (2014) 380–392.

[6] A. S. Avestimehr, D. N. C. Tse, Outage capacity of the fading relay channel in the low-SNR regime, IEEE Trans. Inform. Theory 53 (4) (2007) 1401–1415.

[7] N. C. Beaulieu, J. Hu, A closed-form expression for the outage probability of decode-and-forward relaying in dissimilar Rayleigh fading channels, IEEE Commun. Lett. 10 (12) (2006) 813–815.

[8] T. Nechiporenko, K. T. Phan, C. Tellambura, H. H. Nguyen, On the capacity of Rayleigh fading cooperative systems under adaptive transmission, IEEE Trans. Wireless Commun. 8 (4) (2009) 1626–1631.

[9] P. Ju, W. Song, D. Zhou, Survey on cooperative medium access control protocols, IET Communications 7 (9) (2013) 893–902.

[10] P. Nain, D. Towsley, B. Liu, Z. Liu, Properties of random direction models, in: Proc. IEEE INFOCOM, Vol. 3, 2005, pp. 1897–1907.

[11] D. Stoyan, W. S. Kendall, J. Mecke, Stochastic Geometry and Its Applications, John Wiley & Sons, 1995.

[12] M. Haenggi, J. G. Andrews, Fran, F. Baccelli, O. Dousse, M. Franceschetti, Stochastic geometry and random graphs for the analysis and design of wireless networks, IEEE J. Select. Areas Commun. 27 (7) (2009) 1029–1046.

[13] J. N. Laneman, D. N. C. Tse, G. W. Wornell, Cooperative diversity in wireless networks: Efficient protocols and outage behavior, IEEE Trans. Inform. Theory 50 (12) (2004) 3062–3080.

[14] P. A. Anghel, M. Kaveh, Exact symbol error probability of a cooperative network in a Rayleigh-fading environment, IEEE Trans. Wireless Commun. 3 (5) (2004) 1416–1421.

[15] S. Ikki, M. H. Ahmed, Performance analysis of cooperative diversity wireless networks over Nakagami-m fading channel, IEEE Commun. Lett. 11 (4) (2007) 334–336.

[16] H. A. Suraweera, P. J. Smith, J. Armstrong, Outage probability of cooperative relay networks in Nakagami-m fading channels, IEEE Commun. Lett. 10 (12) (2006) 834–836.

[17] S. S. Ikki, M. H. Ahmed, Performance analysis of generalized selection combining for amplify-and-forward cooperative-diversity networks, in: Proc. IEEE ICC, 2009.

[18] G. Amarasuriya, M. Ardakani, C. Tellambura, Output-threshold multiple-relay-selection scheme for cooperative wireless networks, IEEE Trans. Veh. Technol. 59 (6) (2010) 3091–3097.

[19] W. Zhuang, M. Ismail, Cooperation in wireless communication networks, IEEE Wireless Communications 19 (2) (2012) 10–20.

[20] W. Zhuang, Y. Zhou, A survey of cooperative mac protocols for mobile communication networks, Journal of Internet Technology 14 (4) (2013) 541–560.

[21] D. Yang, X. Fang, G. Xue, HERA: An optimal relay assignment scheme for cooperative networks, IEEE J. Select. Areas Commun. 30 (2) (2012) 245–253.

[22] H. Shan, H. Cheng, W. Zhuang, Cross-layer cooperative MAC protocol in distributed wireless networks, IEEE Trans. Wireless Commun. 10 (8) (2011) 2603–2615.

[23] X. Zhang, J. Tang, Power-delay tradeoff over wireless networks, IEEE Trans. Commun. 61 (9) (2013) 3673–3684.

[24] J. Choi, Energy-delay tradeoff comparison of transmission schemes with limited CSI feedback, IEEE Trans. Wireless Commun. 12 (4) (2013) 1762–1773.

[25] Z. Gong, M. Haenggi, Interference and outage in mobile random networks: Expectation, distribution, and correlation, IEEE Trans. Mobile Comput.

[26] F. Baccelli, B. Blaszczyszyn, P. Muhlethaler, An Aloha protocol for multihop mobile wireless networks, IEEE Trans. Inform. Theory 52 (2) (2006) 421–436.

[27] F. Baccelli, B. Blaszczyszyn, P. Muhlethaler, Stochastic analysis of spatial and opportunistic Aloha, IEEE J. Select. Areas Commun. 27 (7) (2009) 1105–1119.

[28] R. K. Ganti, M. Haenggi, Analysis of uncoordinated opportunistic two-hop wireless ad hoc systems, in: Proc. IEEE International Symposium on Information Theory, 2009, pp. 1020–1024.

[29] C. Zhai, W. Zhang, G. Mao, Uncoordinated cooperative communications with spatially random relays, IEEE Trans. Wireless Commun. 11 (9) (2012) 3126–3135.

[30] A. Jin, W. Song, P. Ju, D. Zhou, An energy-efficient uncoordinated cooperative scheme with uncertain relay distribution intensity, IEEE Trans. Veh. Technol.Accepted, 2014.

[31] A. Goldsmith, Wireless Communications, 1st Edition, Cambridge, 2005.

[32] M. S. Gokturk, O. Ercetin, O. Gurbuz, Throughput analysis of ALOHA with cooperative diversity, IEEE Commun. Lett. 12 (6) (2008) 468–470.

[33] Y. W. P. Hong, C. Lin, S. Wang, Exploiting cooperative advantages in slotted ALOHA random access networks, IEEE Trans. Inform. Theory 56 (8) (2010) 3828–3846.

[34] H. Shan, P. Wang, W. Zhuang, Z. Wang, Cross-layer cooperative triple busy tone multiple access for wireless networks, in: Proc. IEEE GLOBECOM, 2008.

[35] P. J. Davis, P. Rabinowits, Methods of Numerical Integration, 2nd Edition, Academic Press, 1984.

[36] H. Li, Numerical Analysis, 1st Edition, Huazhong University of Science and Technology Press, 2003.